This work was supported in part by the Shanghai Science and Technology Commission: Research and Demonstration under Key Technologies of Multi-Energy Routers (18DZ1203700). *(Corresponding author: Da Xie.)*.

Mingjie Pan and Da Xie are with the Department of Electrical Engineering (the Key Laboratory of Control of Power Transmission and Conversion, Ministry of Education), Shanghai Jiao Tong University, Shanghai 200240, China (e-mail: pmj19971014@sjtu.edu.cn; xieda@sjtu.edu.cn).

Chenlei Wang is with Shanghai Shinan Power Supply Company, Shanghai 200235, China (e-mail: Wangcl@sh.sgcc.com.cn).

Pengfei Ju is with the School of Electrical Engineering, Shanghai Dianji University, Shanghai 200240, China (e-mail: 1521377953@qq.com).

Chenghong Gu is with the Department of Electronic and Electrical Engineering, University of Bath, Bath BA27AY, U.K. (e-mail: c.gu@bath.ac.uk).

Optimal Design and Configuration Strategy for the Physical Layer of Energy Router Based on the Complex Network Theory

Mingjie Pan, Da Xie, *Senior Member, IEEE*, Chenlei Wang, Pengfei Ju, and Chenghong Gu, *Member, IEEE*

***Abstract*—The energy router (ER) is key to realizing the coordinated management and efficient utilization of multiple forms of energy in Energy Internet. This paper proposes a novel design and configuration method for the physical layer of ER by using complex network theory. Firstly, an abstract model of the physical layer of ER is introduced according to its function, and important modules in the model are illustrated in details. Secondly, based on the electrical characteristics of ports, the community structure of the power networks inside ER is analyzed by the improved Girvan-Newman (GN) algorithm to design the independent bus systems (IBSs) and generate the network topology of the physical layer. Then, the optimization model of equipment configuration of the power supply and distribution systems of ER is developed considering the economy, utilization efficiency, and power supply reliability. Finally, two case studies demonstrate that the proposed strategy can effectively accomplish the module-level structure design and device configuration for the physical layer of ER.**

***Index Terms*—Physical layer of energy router, the complex network theory, structure design, optimal configuration strategy.**

I. INTRODUCTION

WITH the acceleration of global industrialization, the energy problem has become an important issue in social and economic development [1]. Replacing traditional fossil fuels with renewable energy to upgrade the energy structure is an inevitable requirement for building high-quality modernized economy and improving the environment [2]. In this context, the Energy Internet (EI), with the help of Internet thinking, transmits and utilizes distributed electricity, natural gas, thermal energy and other forms of energy in an integrated system, which can effectively increase the utilization proportion of renewable energy resources and reduce the comprehensive cost of energy services [3]-[5].

Similar to the role of the information router in the Internet, energy router (ER), also known as the power router [6] and digital grid router [7], can achieve efficient and hybrid utilization of various energy, accommodate high proportion of renewables and guarantee the stable operation of the traditional power grid. So ER is the core equipment for building EI [8]. With a more secure, efficient and sustainable mode of energy utilization, ER has good advantages in power quality control [9], hybrid AC-DC distribution [10], active management of bidirectional power flow [11], convenient access to distributed sources [12] and energy management optimization [13], and has attracted more researchers' attention.

The current research on ER mainly focuses on two aspects: 1) modeling the input-output (I/O) characteristics and coupling relationships of energy in ER based on the conceptual model of energy hub (EH) [14], and applying the above model to the planning and operation of multi-energy systems (MES) [15]-[17]; 2) designing power conversion modules based on power electronic technology [18], or studying energy management and operation control strategies of ER based on a defined topology [19]-[23]. Liu T *et al.* [14] modeled the nodal I/O characteristics of the operating devices in EH and optimized the operation. Zhou *et al.* [15] proposed the concept of virtual energy router (VER), and planned the equipment capacity and network routing for multi-area MES containing multiple ERs. Xu *et al.* [16] considered EHs as nodal decision-makers and proposed a distributed multi-cycle multi-energy operation model for MES. Guo *et al.* [17] introduced a bi-level dispatch strategy to reduce the complexity of large-scale centralized optimization as well as protect the information privacy of different users. Li *et al.* [18] designed a multi-unit reconfigurable architecture with multi-input multi-output (MIMO) power conversion for multi-port applications such as multi-source ER, battery balancers and PV optimizers. Chen *et al.* [19] modeled flexible power loads and energy storage as stochastic processes, and proposed an energy management strategy for ER based on Lyapunov optimization. Liu Y *et al.* [20] proposed a hierarchical control strategy for ER based on fuzzy logic with the help of switching array modules and bidirectional DC/AC converters, which can achieve plug-and-play access and reliable energy management for consumers. Liu B *et al.* [21] studied an AC-DC hybrid multi-port ER structure and developed a corresponding coordinated control strategy to ensure the proper operation of ER. Hussain *et al.* [22] developed an IEC 61850 communication-based power routing algorithm to dynamically control and optimize energy flow in EI. Sosnina *et al.* [23] integrated the artificial neural network into the decentralized ER control system.

However, both types of above research are difficult for a wide range of production and engineering practices for ER. The former regards ER as an energy control unit rather than a physical equipment, and the derived extra-functional properties of ER cannot guide the design of its internal power networks; the latter usually develops structure and components of ER for specific targets, which only have a single function and no generality. In the context of the future EI, ER needs to realize the functions of plug-and-play for devices, centralized energy management, voltage transformation and demand response within multi-energy networks [24]. This requires that the ER should exhibit a flexible and extensible structure at the physical layer to achieve a rich variety of functions. In other

words, manufacturers should be able to select standardized and modular components to integrate generic modules according to users' requirements, and eventually customize them into personalized ER equipment for utilization.

All primary energy sources as well as clean and efficient secondary energy sources can both be converted into electric energy, and most end-use energy consumption can also be replaced by electric energy. At the same time, electric energy requires a power balance at all times and has the shortest time scale. As a result, electric energy is the core of ER, and efficient and flexible power networks are the core architecture of the physical layer of ER [25]. This paper focuses on the overall structure design of the power networks of ER's physical layer. The network topology inside ER can be manifested as the electrical connections between ports, energy transmission and conversion devices, and IBSs, which can be abstracted as the connection relationships between nodes and the affiliation relationships between nodes and clusters. The complex network theory, as a mathematical theory that analyzes connection relations, can well solve the above problem. Power networks have the properties of self-organization, self-similarity, small world, scale-free and community structure, which are typical complex networks. Therefore, the complex network theory can represent the cyber-physical fusion features of power networks, reflect the characteristics of energy inter-connection, and apply to modelling power networks [26]-[28].

To fill the research gap and provide guidance for designing and producing physical ER equipment, this paper proposes a generic model of ER's physical layer, translates the topology design problem based on the complex network theory, and finally realizes the design and optimization of power networks of ER's physical layer. The main contributions are as follows:

1) A module-level generic model of ER's physical layer that takes into account both the extra-functional and internal circuit characteristics of ER is proposed. The model expresses a high degree of abstraction of the devices and components at the physical equipment level.

2) The physical layer topology of ER is viewed from the perspective of the complex network theory, and the design of IBSs is transformed into a community division problem. The design quality is evaluated by modularity to obtain optimal topology, which greatly reduces the difficulty of module-level design.

3) The optimization model of device configuration enables manufacturers to evaluate the operational performance of ER at the design stage. The proposed three indicators of the economy, efficiency, and reliability can comprehensively reflect EI's requirements of clean, efficient and safe energy use.

4) The proposed design and configuration strategy has a wide range of applications and can be flexibly extended to scenarios with different functions and purposes, which is applicable to both single-area and multi-area systems.

The remainder of this paper is organized as follows. Section II introduces the concept, model, and typical structure of the physical layer of ER. Section III studies the construction of the complex network for ER's physical layer considering the port electrical characteristics, and designs the IBSs based on the improved GN algorithm. The optimization model of device configuration is given in Section IV. Section V selects two case studies to verify the effectiveness and applicability of the proposed design and configuration strategy. Brief conclusions are drawn in Section VI.

II. Model of the Physical Layer of ER

This section presents the concept and model of the physical layer of ER and is the theoretical basis for the research.

A. Concept of the Physical Layer of ER

The ER is a multi-level distributed energy interconnection system with power networks as the backbone, integrating power electronic conversion technology and information technology to realize extensive energy sharing and storage. The power electronic conversion technology enables ER to provide the required electrical ports for various types of distributed power sources, energy storage devices, multi-energy coupling devices, and loads. The information technology enables the hybrid AC/DC micro-grid managed by ER both to implement self-regulated operation and to serve as an interactive interface to the external grid, responding to the upper-level dispatch center to achieve optimal operation. The cyber-physical fusion architecture of ER with electric energy as the core is shown in Fig. 1(a).

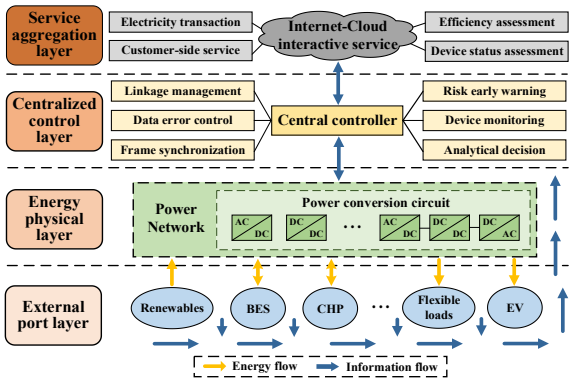

(a) Cyber-physical fusion architecture

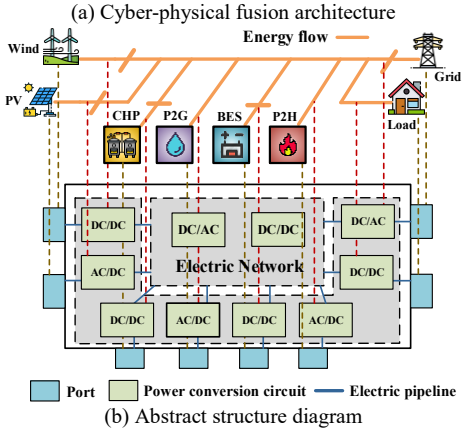

(b) Abstract structure diagram

Fig. 1. Physical layer of ER with electric energy as the core.

The physical layer of ER should be designed as a modular structure, including three main parts: standardized electrical

ports, independent bus systems, and power conversion circuit collection. Externally, ER equals to different energy ports in a "plug-and-play" form. ER can be seen as a "black box" where distributed energy sources and energy conversion devices are connected in the form of electric energy through the "plug-and-play" ports. The port device is not concerned with the complex coupling relationships between different energy sources within the system, but only needs to ensure the energy state of the port. Internally, ER acts as interconnected power networks consisting of IBSs and power conversion circuits. Through the combination of converters in different operating modes, ER achieves the unified transmission, storage and forwarding of energy. Simultaneously, the whole ER system aggregates and distributes electric energy by extending and interconnecting to each port through independent buses.

Therefore, the architecture in Fig. 1(a) can be abstracted as a schematic diagram of the physical layer structure of ER based on the standardized electrical ports, independent bus systems, and power conversion circuits in Fig. 1(b).

B. Abstract Model of the Physical Layer of ER

1) Standardized Electrical Ports: The standardized ports provide "plug-and-play" energy access for generation and consumption devices, and can automatically scan the operating information to identify the state of various port devices. Each type of grid-connected equipment connected to ER operates according to the goal set by each part, such as photovoltaic (PV) and wind power according to the maximum power generation. The ER fulfills the information interaction between each part and itself through information collection and transmission devices, and performs port energy control as well as energy routing through the internal power networks.

2) Independent Bus Systems: The concept of IBS in ER is introduced to enhance the flexibility of ER's structure while ensuring supply reliability. Multiple IBSs are set up to ensure reliable operation depending on the practical requirements. IBSs of the same voltage level are represented as segmented buses or physically are converted from IBSs of other voltage levels. The independent buses inside ER are divided into the two following categories.

(1) Independent DC Bus (IB_{DC}): DC buses are the core and foundation of IBS. The power supply systems of ER with IB_{DC} as the core can facilitate the flexible access of generating units, energy storage, loads, etc., and can also give full play to the energy buffer effect of DC buses to maximize the utilization rate of distributed renewables. Also, in DC systems, the only criterion to measure the active power balance is the bus voltage, and there are no power quality problems such as frequency stability and reactive power compensation in the AC grid, ensuring the transmission of high-quality power.

(2) Independent AC Bus (IB_{AC}): AC buses are set up to provide ports mainly for the internal AC loads in the system. IB_{AC} is inverted by IB_{DC} and is not connected to the external grid. The IB_{AC} systems are highly flexible and variable. Through the control of the inverters, the frequency, voltage, phase sequence and other operating conditions of IB_{AC} can be changed to meet the diverse power supply needs of the loads, which facilitates the energy management of ER.

3) Collection of Power Conversion Circuits: There are two types of converters in ER: DC/DC converters and AC/DC converters, which play the role of energy conversion and voltage conversion. The power conversion circuits inside ER collect the information about the energy state. Such information is then fused to generate control signals to achieve the regulation of the energy flow. In addition, most of the ports in an open interconnected ER should have the characteristics of bi-directional power flow.

C. Typical Structure of the Physical Layer of ER

Fig. 2 shows the typical structure of single independent bus system and dual independent bus system of ER. Although the two structures have similar external ports, their design and operational control are quite different.

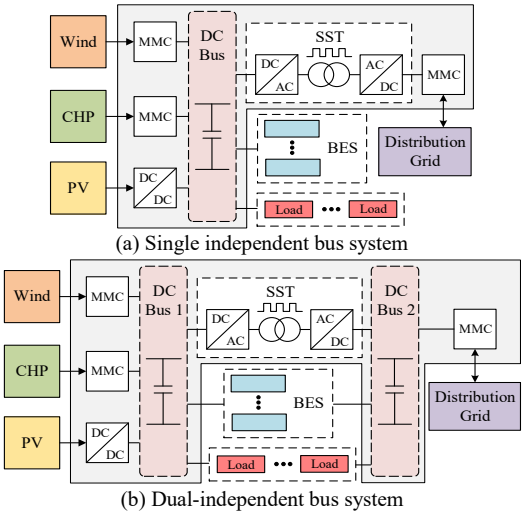

Fig. 2. Typical structure of the physical layer of ER.

In Fig. 2(a), the voltage stability of the IB_{DC} is key to the stable operation of ER. The voltage stability requirement of the single IB_{DC} system indicates both the balance of energy supply and demand and the operating constraints inside ER. However, at this time, all ports of fluctuating renewables, energy conversion devices and loads are connected to the same DC bus. The safe and stable operation of the system requires precise and reliable control of each port, which makes it difficult to maintain the bus voltage. The collapse of the bus voltage will make all ports out of control, so the reliability of the whole system is relatively poor.

In contrast, in the dual-independent bus system shown in Fig. 2(b), the voltages of the two DC buses are different. Thus, it is possible to either connect the two DC bus systems through converters or disconnect them to form two different power supply systems that operate independently according to the actual situation. For example, the output of PV and wind power ports might be affected by volatility in solar radiation, temperature or wind speed. At this time, the converter between two buses can be blocked, while the load is connected at the end of the grid-side bus, limiting the fluctuation of the bus at the side of fluctuating renewable energy on DC Bus 1.

With the rapid development of fluctuating renewables,

flexible loads and multi-energy coupling devices, the number of energy production, consumption and storage components in EI has increased significantly, requiring ER to evolve from a simple system with only three ports of "source-load-storage" to a complex multi-port system. Each port may have different voltage level and power form, which inevitably requires multiple buses to match.

Among them, the number of independent buses becomes a key factor for the physical layer configuration of ER. Too many or too few independent buses will affect the safe and economic operation. If the number of independent buses is too few, on the one hand, the correlation between different ports is strong, so once a port has power fluctuation or the converter connected to the port fails, the normal operation of the considerable ports belonging to the same independent bus will be affected, and the reliability of the system will be reduced; on the other hand, the operating conditions available to the system are limited, the energy flow path becomes more difficult to control, and the system may not operate at the optimal economic point. Conversely, too many independent buses augment the structure complexity, which greatly increases the configuration cost and difficulty, and puts higher requirements on the control system.

Therefore, it is crucial for the stable and efficient operation of ER to reasonably divide its ports into several clusters using a suitable theory based on the electrical characteristics of each port to form the corresponding IBSs.

III. Design Strategy for Physical Layer Topology of ER Based on the Complex Network Theory

In this section, the physical layer topology of ER is designed based on the complex network theory. Firstly, the ER system is modeled as complex network and the basic topology is formed by calculating the electrical similarity between nodes. Then the "community" concept is used to describe the IBS, and the design of IBSs is transformed into a community division problem solved by an improved GN algorithm. As a result, the nodes with similar electrical characteristics are classified into the same community. Finally, a suitable bus voltage is selected to configure the formed community as an IBS.

A. Initial Networks Based on Port Electrical Characteristics

1) Mapping Relationship Between Electrical Physical Layer and Complex Networks: The ports in ER's power networks have different electrical characteristics and there are complex linkage relationships between them, making the ER a typical complex system. The Complex network based on electrical characteristics is a topology diagram that reflects the electrical relationships of energy conversion, transmission and storage devices within ER. Relevant concepts involved are defined in Table I and the typical nodes in ER are shown in Table II.

TABLE I
RELEVANT CONCEPTS IN THE COMPLEX NETWORK THEORY

Name	Explanation
Node	Nodes are the basic units that compose the networks. The nodes correspond to energy conversion devices, energy storage devices, and electrical loads of each port in ER at the physical layer.
Edge	The links between the nodes form the edges of the networks and represent the electrical connections. Edges correspond to energy transmission devices and converters at the physical layer.
Network	Networks are a topology consisting of nodes and edges. The structure of the networks reflects the aggregation and group state of the electrical devices inside ER.
Small world feature	The small-world feature means that most of the nodes in the networks are not adjacent to each other, but they can reach any other node in a few steps. In the power networks of ER, this property means that only a limited number of steps are required for energy flow between ports.
Scale-free feature	The scale-free feature means that most of the nodes in the networks are connected to very few nodes, while a very small number of nodes are connected to plenty of nodes. In the power networks of ER, high-power conversion circuits are configured at such nodes to achieve electrical connections between different independent buses.

TABLE II
CLASSIFICATION OF NODES IN POWER NETWORKS OF ER

Type	Nodes included
Source (Ω_S)	PV, wind power, combined heat and power (CHP) unit, power grid, etc.
Energy Storage (Ω_B)	Battery energy storage (BES)
Load (Ω_L)	AC load, DC load

2) Description of Port Electrical Characteristics: The three factors of power supply/consumption category, voltage level, and power characteristics are used to describe the electrical characteristics of the port devices. The electrical similarity $ES(i,j)$ describes the agreement of the electrical characteristics of nodes i and j, which is expressed as follows.

$$ES(i,j)=\alpha_C\cdot ES_C(i,j)+\alpha_V\cdot ES_V(i,j)+\alpha_P\cdot ES_P(i,j) \quad (1)$$

$$\alpha_C+\alpha_V+\alpha_P=1 \quad (2)$$

$$ES_C(i,j)=h(CA_i)\odot h(CA_j) \quad (3)$$

$$ES_V(i,j)=1-\frac{|V_i-V_j|}{V_{\max}-V_{\min}} \quad (4)$$

$$ES_P(i,j)=\begin{cases} R(P_i,P_j) & i,j\in\Omega_S \text{ or } i,j\in\Omega_L \\ 1 & i,j\in\Omega_B \\ 0 & otherwise \end{cases} \quad (5)$$

$$R(a,b)=\frac{\mathrm{cov}(a,b)}{\sqrt{\mathrm{var}(a)\,\mathrm{var}(b)}} \quad (6)$$

where $ES_C(i,j)$, $ES_V(i,j)$ and $ES_P(i,j)$ are the similarity of power supply/consumption category, voltage level, and power characteristics of nodes i and j, respectively; α_C, α_G and α_P are their similarity coefficients; $CA_i(CA_j)$, $V_i(V_j)$ and $P_i(P_j)$ denote the power category, operating voltage, and active power curve of node $i(j)$, respectively; h is a Boolean variable, whose value 1/0 represents the node voltage in the form of AC/DC; $\odot$ is the XNOR operator; $V_{\max}$ and $V_{\min}$ are the maximum and minimum values of the operating voltage of all nodes; the similarity of power characteristics is calculated using serial correlation, $R(a,b)$ denotes the correlation coefficient of series a and b, cov is the covariance and var is the variance.

α_C, α_G and α_P indicate the weights of the power supply/consumption category, voltage level, and power characteristics in calculating the electrical similarity of nodes, respectively. The ER designer can set different values of the three parameters to form different basic topologies of power networks according to the requirements. It can be seen from (1)-(6) that the voltage levels of the port devices play a major role when the

weights are close. In addition, the source-side nodes are distinguished from the load-side nodes due to the consideration of the power category and the node power characteristics.

3) Generation of Initial Networks: In the complex networks mapped from the electrical physical layer of ER, an edge between two nodes represents that they have similar electrical characteristics. By setting different thresholds and connecting nodes with a similarity greater than this threshold, diverse initial topologies of power networks can be obtained.

A community is a combination of individuals in complex networks who behave similarly, are closely connected, or have the same interests. Therefore, complex networks can also be considered as the collection of multiple communities. On this basis, applicable clustering algorithms can be used to find the communities in the networks, and nodes with similar electrical characteristics are classified into the same community, which can provide a reference for the design of IBSs.

B. Community Division Based on Improved GN Algorithm

1) Basic GN Algorithm: The GN algorithm is a classical divisive method proposed by Girvan and Newman for finding the community structure in complex networks [29]. Its basic idea is that one or more shortest paths exist between any two nodes, and if most of the shortest paths include a certain edge, then there are relatively few other paths between the nodes at both ends of that edge, and these two nodes can be grouped into two communities. Two important concepts in the GN algorithm are betweenness and modularity.

(1) Betweenness: The betweenness $Bet(i,j)$ of the edge with nodes i and j as endpoints in graph G is defined as the number of shortest paths passing through this edge in the networks. The betweenness reflects the influence of the corresponding edge in the whole networks and is calculated in (7).

$$Bet(i,j)=\sum f(l,i,j) \quad \forall l \in L_m; i,j \in G \tag{7}$$

where l is a certain shortest path, L_m is the set of shortest paths in graph G; f is the judgment function, whose value is 1 when l passes through the edge of nodes i and j, and 0 otherwise.

(2) Modularity: Modularity Q is a measure of the quality of network division [30]. The closer its value is to 1, the stronger the strength of the community structure of the networks, i.e., the better the quality of division. Therefore, the optimal community division of the networks can be obtained by maximizing Q. The power networks of ER are regarded as weighted networks and the modularity is calculated by (8).

$$\begin{cases} Q=\dfrac{1}{2M}\sum\limits_{i,j\in G}\left(a_{ij}-\dfrac{k_i k_j}{2M}\right)\delta(\sigma_i,\sigma_j) \\ M=\dfrac{1}{2}\sum\limits_{i,j\in G}a_{ij} \end{cases} \tag{8}$$

where M is the sum of the edge weights in the networks; a_{ij} is an element in the adjacency matrix of the networks, and it is the edge weight if nodes i and j are connected, otherwise it is 0; k_i and k_j are the degrees of nodes i and j, respectively; $\delta(\sigma_i,\sigma_j)$ is the membership function, whose value is 1 when node i and j belong to the same community, and 0 otherwise.

In the power networks of ER, the edge weight is defined according to the construction cost of the energy transmission equipment, which is calculated in (9).

$$a_{ij}=\frac{C_{0,l}L_{ij}}{\min\{C_{0,l}L_{ij}\}} \tag{9}$$

where $C_{0,l}$ is the construction cost of per unit length of energy transmission equipment; L_{ij} is the line length between nodes i and j; $\min\{C_{0,l}L_{ij}\}$ is the minimum value of cost among all lines to be constructed.

2) Improved GN Algorithm: The basic GN algorithm does not consider the node weight, which may cause the size of each subgraph after division to vary widely and the algorithm to be trapped in the local optimum. Thus, improvement is made by considering the contribution of the nodes to the modularity. The contribution value q_i of node i to Q is defined in (10).

$$q_i=k_{r(i)}-k_i a_{r(i)} \tag{10}$$

where $k_{r(i)}$ is the number of the edges between node i and other nodes within community r; $a_{r(i)}$ is the proportion of edges connected to node i to all edges in the whole networks.

To be consistent with the modularity, the range of q_i should also be kept in the range of 0 to 1. So q_i is normalized in (11).

$$\lambda_i=\frac{q_i}{k_i}=\frac{k_{r(i)}}{k_i}-a_{r(i)} \tag{11}$$

Then the contribution of nodes to the modularity Q is added as their weights to the original formula for calculating the betweenness, as shown in (12).

$$Bet'(i,j)=\frac{Bet(i,j)}{\lambda_i+\lambda_j} \tag{12}$$

Calculating the betweenness based on the node weight can change the order of cutting edges, which in turn can change the results of the network division, making the divided subgraphs more reasonable. The specific description of the improved GN algorithm is shown in Table III.

TABLE III
DESCRIPTION OF IMPROVED GN ALGORITHM

Algorithm1: Improved GN algorithm based on node weight

Input: Node electrical characteristics, similarity threshold ES_t
Initialization: node set N, adjacency matrix A, node degree K
Main program:
```
Calculate the equation (1)-(5) to get electrical similarity ES;
for node i ≠ j in N:
    if ES(i,j) > ES_t:
        put an edge between node i and j;
Form the graph G, calculate matrix A;
Repeat:
    Calculate the betweenness of each edge Bet(i,j) by BFS algorithm;
    for (i,j) in Bet:
        if Bet(i,j) == max(Bet.values()):
            G.remove_edge(i,j);
        end
    for i ≠ j in G:
        Q = Q + (a_ij - k_i*k_j/2M)/2M;
    end
Until G.number_of_edges() == 0.
```

C. Design of IBSs Based on Network Communities

The idea of community division in which individuals with similar characteristics in a group are classified into the same community is consistent with the nature and goal of ER's

design problem of connecting ports with similar electrical characteristics to the same independent bus. Therefore, it can be considered that modularity can also be used as a quantitative indicator to characterize the quality of IBS. Thus, the optimal topology can be obtained by solving the community structure with the maximum modularity in ER's corresponding complex networks.

During the formation of the power networks based on the complex network theory, the electrical devices with similar characteristics gather into clusters and converge into a group under the same power supply system. Thus, a community can be considered as an IBS inside ER. After dividing the power networks into several communities, the corresponding number of IBSs is obtained. Then it is necessary to determine the type and the voltage level of each independent bus.

Compared with AC systems, DC power supply systems have advantages such as low line loss, good power quality, high operational efficiency, convenient access to renewable energy generation, etc., which can provide safe, flexible and efficient power supply services. Therefore, the power supply and distribution systems inside ER should be mainly DC systems, and the access of ports should be mainly to IB_{DC}.

The voltage levels of IBSs should be set based on engineering experience. Common bus voltage levels are given in Table IV and they form the alternative set. The voltage of each IBS is selected from the set and the value is close to the average voltage of the ports that it is connected to. Because ER is a piece of active equipment and the voltages of its independent buses are decided by the control of power electronic converters, the voltages of internal independent buses can be set without power flow calculation. In addition, when designing a multi-area ER system, each area should be configured with an additional converter to the high voltage to facilitate the construction of transmission lines.

TABLE IV
COMMON BUS VOLTAGE LEVELS

Bus type	Voltage level (V)
DC bus	48, 240, 375, 540, 750, 1500
AC bus	220, 380

IV. EQUIPMENT CONFIGURATION STRATEGY FOR THE PHYSICAL LAYER OF ER

A. Optimization Model for Equipment Configuration

Each port of ER is connected to the independent bus of the community to which it belongs through energy transmission devices and power conversion circuits, and the independent buses can also be connected through converters. Thus, the optimal structural design can be achieved by rational selection of the power conversion circuits and the design of the liaison relationships between the independent buses.

1) Objective Function: Engineering economy is the primary factor to be considered in the equipment configuration at the physical level. Additionally, ER efficiently utilizes distributed renewable energy through the coordinated management of multiple energy forms, so the energy loss in the operation process should also be considered. Furthermore, the design of the power networks should ensure the safe and reliable operation of power supply and distribution systems. As a result, economy, efficiency, and reliability are chosen as the three indicators for configuration objectives.

(1) The economic optimum is equivalent to the lowest cost, including investment and construction cost C_{inv}, and operation and maintenance cost C_{ope}.

$$\min f_1 = C_{inv} + C_{ope} \tag{13}$$

$$C_{inv} = \frac{r(1+r)^T}{(1+r)^T - 1}\left[\sum_{i\in N} C_{i,con} + \sum_{j\in\Phi}\sum_{k\in\Phi} x_{jk} C_{jk,con}\right] \tag{14}$$

$$C_{ope} = \sum_{i\in N} C_{i,man} + \sum_{j\in\Phi}\sum_{k\in\Phi} x_{jk} C_{jk,man} + \sum_{i\in N} C_{i,tra} \tag{15}$$

where r is the annual discount rate; T is the lifespan; N is the node set; $C_{i,con}$, $C_{i,man}$ and $C_{i,tra}$ are the construction cost and fixed maintenance cost of the power conversion circuit, and the operating cost at node i, respectively; Φ is the set of independent buses; x_{jk} is a Boolean variable, whose value is 1/0 when there is/is not an energy transmission channel between bus j and bus k; $C_{jk,con}$ and $C_{jk,man}$ are the construction cost and fixed maintenance cost of the energy transmission devices and converters between bus j and bus k, respectively.

(2) The energy utilization efficiency is described by the total energy loss E_{loss} of the system over time. The highest efficiency means the lowest total loss.

$$\min f_2 = E_{loss} = \sum_{i\in N}\sum_{j\in N} y_{ij} \int_{t\in T_w} P_{loss,ij}(t)\mathrm{d}t \tag{16}$$

$$P_{loss,ij}(t) = \begin{cases} \left(1-\eta_{cvt}(t)\right)\eta_{pip} P_{tra}(t) & P_{tra}(t) \ge 0 \\ \left(1/\eta_{cvt}(t) - 1\right)\eta_{pip} P_{tra}(t) & P_{tra}(t) < 0 \end{cases} \tag{17}$$

where y_{ij} is a Boolean variable, whose value is 1/0 when there is/is not an energy transmission channel between nodes i and j; T_w is the set of operating times under study; $P_{loss,ij}(t)$ is the power loss between nodes i and j at time t; $\eta_{cvt}(t)$ is the transmission efficiency of the power conversion circuit at time t, which is calculated from its efficiency curve (loss characteristics); η_{pip} is the average transmission efficiency of the energy transmission pipeline, which is a constant related to the pipeline type; $P_t(t)$ is the power transmitted by the converter at time t. In (17), the power flow from power-side or storage-side nodes to load-side nodes is defined as positive.

(3) The internal power networks inside ER are a supply and distribution system in which we focus on whether the electricity demands of users (loads) are met. The average service availability index (ASAI) can measure supply reliability.

$$\max f_3 = \mathrm{ASAI} = \frac{\sum_{i\in L} 8760 N_i - \sum_{i\in L} U_i N_i}{\sum_{i\in L} 8760 N_i} \tag{18}$$

where L is the set of load nodes; N_i and U_i are the number of users and the annual average interruption time at node i, and the latter is calculated by Monte Carlo simulation (details in Section IV-B).

2) Constraints: The constraints mainly include component and power flow constraints.

$$\begin{cases} f(N) = 0 \\ g(N) \le 0 \end{cases} \tag{19}$$

where $f(N)$ represents the power balance in the system, which is shown in (20), and the component constraint $g(N)$ is shown in (21).

$$\sum P_{gen}(t)=\sum P_{load}(t)+\sum P_{\mathrm{BES}}(t)+\sum P_{loss}(t) \tag{20}$$

where $P_{gen}(t)$, $P_{load}(t)$, $P_{\mathrm{BES}}(t)$ and $P_{loss}(t)$ denote the power generated by sources, consumed by loads, absorbed by energy storage and lost at time t, respectively. P_{gen}, P_{load} and P_{BES} are obtained from day-ahead operation curves. P_{loss} is calculated by (17). For the multi-area system, the efficiency of the transmission lines between different regions is equated with a constant η_{pip}. To improve the accuracy of results, the power transmission loss between regions can be calculated by solving the power flow model [31], but this will also increase the calculation amount of the proposed model.

$$\begin{cases} V_{h,k} \le V_{k\max} \\ \tau_{cvt,k} \le \tau_{k\max} \\ P_{tra,k}(t) \le Cap_k \end{cases} \tag{21}$$

where for converter k, $V_{h,k}$ is the voltage of the high-voltage side and is determined by comparing the voltages of the port and bus to which it is connected, $V_{k\max}$ is the maximum withstand voltage, $\tau_{cvt,k}$ is the voltage conversion ratio, $\tau_{k\max}$ is the maximum voltage conversion range; $P_{t,k}(t)$ is the power transmitted at time t, and Cap_k is the configured capacity.

B. Solution Method of Power Supply Reliability

The Monte Carlo simulation is used to sample the operating state durations of the ports on the source side and the storage side as well as the conversion circuit to obtain the state and duration of the whole system, on which the reliability index is calculated [32], [33].

The work-failure two-state model is used to model each component. Assuming that the failure rate and repair rate of the components are constant λ and μ, respectively, the mean time between failure (MTBF) τ_1 and mean time to repair (MTTR) τ_2 of the components are random variables subject to an exponential distribution, which can be sampled according to (22). Then a sequence of operating state durations of each component is formed and the system state can be obtained.

$$\tau_1=-\frac{1}{\lambda}\ln\delta_1 \qquad \tau_2=-\frac{1}{\mu}\ln\delta_2 \tag{22}$$

where δ_1 and δ_2 are random numbers uniformly distributed in the interval [0,1], respectively.

C. Overall Procedures for Design and Configuration of the physical layer of ER

In summary, the procedures of designing and configuring the physical layer of ER are shown in Fig. 3. Under the condition that the electrical parameters of port devices are known, the main objective is to obtain the optimal module-level topology and equipment configuration. To reduce the complexity of the problem, the overall design process is divided into two stages. In the first stage, the physical layer of ER is mapped into complex networks based on the electrical connections, and the number of independent buses and the connection relationships between ports and buses are obtained by solving the community division problem through the improved GN algorithm. In the second stage, the types and capacities of the converters and transmission lines in the ER system are configured by pursuing multiple goals of economy, efficiency, and reliability. It should be noted that the optimization model of equipment configuration is a typical nonlinear multi-objective problem, which is solved by a multi-objective particle swarm optimizer (MOPSO) [34], [35].

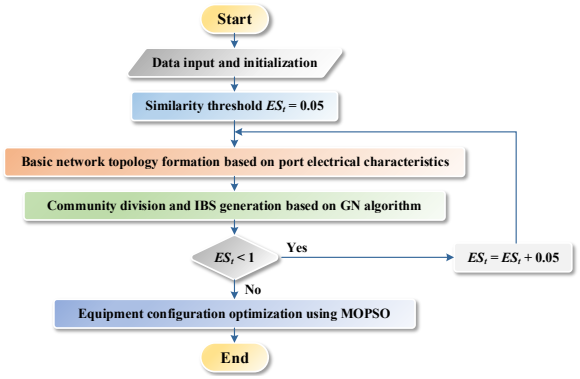

Fig. 3. Flowchart of design and configuration process of the physical layer.

V. Case Study

A. Illustration of Necessary Information

1) Selection of Power Conversion Circuits: In the practical project, different regions and users have different requirements for the functions of the designed ER. To reduce the configuration difficulty, the power supply and distribution components inside ER should have fixed types and uniform standards. It is assumed that all power conversion circuits are packaged modules and the same type of converters have the same parameters including voltage conversion characteristics and efficiency curves.

In this study, five typical power conversion circuits with nine levels of technical maturity and wide application in engineering practice are used to configure the ER system. Their basic parameters and loss characteristics are shown in Table V and Fig. 4. The losses of power conversion circuits composed of power electronics mainly include conduction loss, driving loss and switching loss [36]. The efficiency characteristics is considered for the solid-state transformer (SST) circuit, and β_{T} in Fig. 4(b) is the transformer load ratio [37].

TABLE V
Typical Power Conversion Circuits

Num	Type	Function	Energy flow	Cost (¥/W)
1	Buck or Boost	DC/DC	unidirectional	0.19
2	Buck/Boost	DC/DC	bidirectional	0.23
3	Bridge rectifier/inverter	AC/DC	bidirectional	0.29
4	MMC	AC/DC	bidirectional	0.33
5	SST	DC/DC	bidirectional	1.30

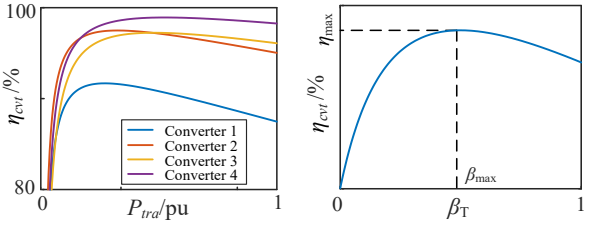

(a) Power electronics circuits (b) SST circuit

Fig. 4. Loss characteristics of power conversion circuits.

2) Reliability Parameters of Components: The reliability parameters of the components that possibly fail are given in Table VI, assuming that the states of different components do not affect each other. Among them, the MTBF of CHP units and transmission lines are obtained according to their failure rates. Also, the MTBF of transmission lines needs to be converted based on their length in the calculation.

TABLE VI
RELIABILITY PARAMETERS OF COMPONENTS

Type	MTBF/h	MTTR/h	Source
Power grid	8030	5	[38]
Normal generating unit	2000	4	[38]
CHP	$2.92*10^5$	200	[39]
BES	$2.4*10^5$	8	[38]
Transmission line	$1.35*10^5$	5	[39]
Buck/Boost	50000	2	[38]
Bridge rectifier/inverter	20000	2	[38]
MMC	$8.4*10^5$	5	[40]
SST	$7.8*10^6$	6	[38]

3) Comparative Analysis of Configuration Strategies: The following three different methods are used to solve the case configuration results for comparative analysis.

Method 1: The method proposed in this paper.

Method 2: Based on the network topology of method 1, use a fixed optimization method based on expert strategies for equipment configuration [41].

Method 3: Using the current conventional design method in power systems. That is all ports are connected directly to the AC bus through power conversion circuits. The equipment configuration method is the same as method 2.

When using methods 2 and 3 to configure the system, the output power of PV equals to the average power of the loads. And all three methods ensure that the capacity of the power conversion circuit at the source node needs to be greater than the sum of the maximum power of all nodes connected to it.

The comparison between methods 1 and 2 aims to show the effectiveness of the proposed optimization model of device configuration, and the comparison between methods 2 and 3 is to demonstrate the superiority of the proposed complex network model in the design of ER's power network structure.

B. Simulation Analysis of Single-area System

1) Case settings: An office building system is chosen as a single-area system case as shown in Fig. 5(a). The equipment parameters and cost factors are given in Table VII. The system has 8 ports: ports 1, 2 and 3 are source nodes, port 4 is an energy storage node, and ports 5 to 8 are load nodes. The data of PV resources and AC/DC loads are selected from the actual engineering data of a typical day, as shown in Fig. 5(b).

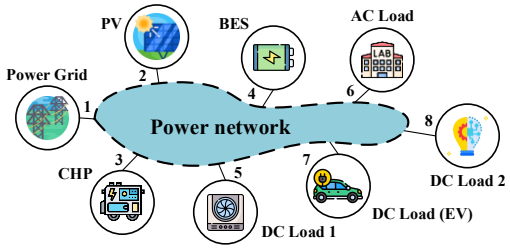

(a) Structure diagram

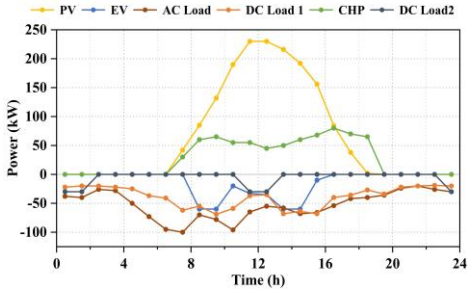

(b) Port characteristics curve

Fig. 5. Illustration of the office building system.

TABLE VII
CONFIGURATION PARAMETERS OF THE BUILDING SYSTEM

Content	Value
Maximum output power of PV	400 kW
Maintenance cost of PV	0.08 ¥/kWh
Capacity of BES	150 kWh
Maintenance cost of BES	0.0018 ¥/kWh
Rated power of CHP	100 kW
Maintenance cost of CHP	0.335 ¥/kWh
Power purchase price at peak time	1.074 ¥/kWh
Power purchase price at valley time	0.671 ¥/kWh

2) Configuration Results: As shown in Table VIII, by continuously removing the edge with the largest betweenness in the networks, the algorithm obtains different community division. The maximum modularity is 0.430 when the number of communities is 4, which means that the system works best when it is divided into four IBSs.

TABLE VIII
RESULTS OF COMMUNITY DIVISION

Number	Modularity	Number	Modularity
1	0.306	5	0.390
2	0.380	6	0.363
3	0.414	7	0.310
4	0.430	8	0

The configuration results are given in Fig. 6. It can be seen that IBS 1, consisting of nodes 2, 4 and 5, is a 750V DC bus system, while the remaining three IBSs in ER are all 375V DC bus systems. Therefore, the IB_{DC} of communities 2, 3 and 4 do not need to configure power conversion circuits in between because their voltage levels are the same. That is, communities 2, 3 and 4 share the same independent bus and their electrical connection with IBS 1 is combined into a single edge, requiring only one converter. Finally, the internal power networks of the whole system take the form of a dual bus system.

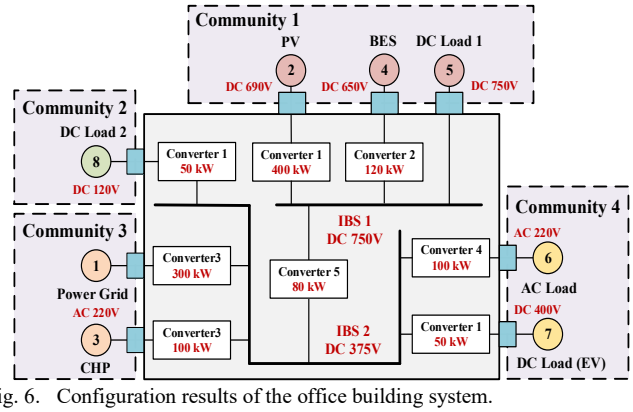

Fig. 6. Configuration results of the office building system.

3) Comparative Analysis: Table IX gives a comparison of the configuration results using the three methods.

TABLE IX
COMPARISON OF CONFIGURATION RESULTS

Method	Cost (*10^4 ¥)		Energy loss (kWh)	ASAI (%)
	Construction	Operation		
1	37.47	2.72	9917.92	99.927
2	39.21	2.76	10336.47	99.935
3	46.83	3.84	13771.76	99.792

The total costs of methods 1 and 2 are few different due to the same topology. The reason for the higher construction cost of method 2 than method 1 is that the capacity of the converter at the BES port in method 2 is slightly larger than that in method 1. In method 3, because all ports will connect to the power grid AC bus, the configuration capacity of the power conversion circuit at the grid port needs to be greater than or equal to the sum of all loads connected to the bus, which makes the construction cost significantly higher.

From the perspective of energy utilization efficiency, IBS 1 and IBS 2 can exchange power through converter 5 in method 1, and the configuration capacity of the BES port converter only needs to consider the exchange power through converter 5 and the power of DC Load 1. Thus, method 1 decreases the converter capacity at the BES port and the grid port, making each converter work near the maximum point of the efficiency curve and reducing the energy loss from system operation.

Concerning power supply reliability, the ASAI values of methods 1 and 2 are similar and greatly higher than that of method 3. This is because methods 1 and 2 have the same power network topology and use dual independent buses for power supply, which has more means to cope with component failures. Method 2 has a larger capacity of the converter on the BES side, which can better satisfy the fluctuation of PV output, making the power supply to DC Load 1 more reliable. In contrast, method 3 has only one IB_{AC} in the system, which will affect all loads in case of failure of important components, and therefore has the lowest reliability of power supply.

C. Simulation Analysis of Multi-area System

1) Case settings: The multi-park energy system in [15] is adopted for multi-area research. It should be noted that the construction of energy transmission equipment at each port should be considered between different regions in this section.

2) Configuration Results: As shown in Table X, the maximum modularity is 0.679 when the networks are divided into 7 communities. That is a total of 14 nodes in these three regions are classified into 7 IBSs.

TABLE X
RESULTS OF COMMUNITY DIVISION

Number	Modularity	Number	Modularity
1	0.547	8	0.658
2	0.585	9	0.643
3	0.597	10	0.624
4	0.632	11	0.609
5	0.655	12	0.532
6	0.664	13	0.351
7	0.679	14	0

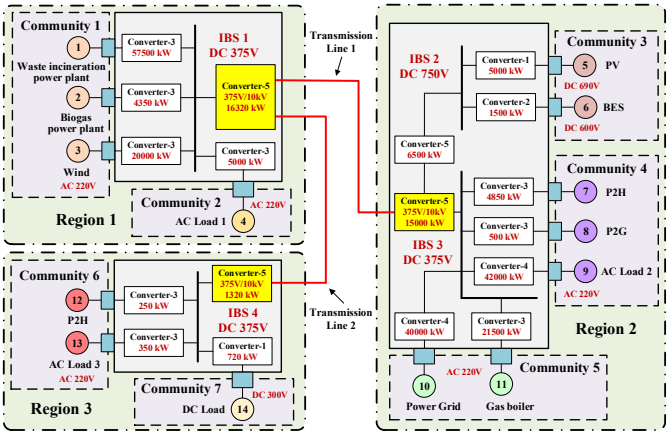

Fig. 7. Configuration results of the multi-park energy local area network.

Fig. 7 presents the overall configuration results of the multi-park system. The designed regional power networks take the 10kV DC network as the backbone and transmits electricity between regions through two overhead lines. The system is a combination of 4 IB_{DC} systems. Regions 1 and 3 use a 375V DC system, and region 2 includes 375V and 750V IB_{DC} systems. For the sake of power transmission, a boost converter with SST as the core is added to each regional ER to increase the voltage to 10kV DC.

3) Comparative Analysis: Table XI gives a comparison of the configuration results using the three methods. The construction cost referred to in this section is the construction cost of the power networks, excluding that of energy devices. Therefore, in the process of establishing a large-scale system, the network construction cost is far less than operation costs.

TABLE XI
COMPARISON OF CONFIGURATION RESULTS

Method	Cost (*10^6 ¥)		Energy loss (MWh)	ASAI (%)
	Construction	Operation		
1	0.4423	24.62	7823.10	99.301
2	0.4487	26.97	8126.47	99.317
3	0.5774	32.14	8744.77	98.896

The operating costs of methods 1 and 2 are close, while that of method 3 is much higher than the former two, which shows that the network topology designed by the strategy proposed in this study can reduce the overall cost of the system. From the efficient point of view, the energy loss of method 1 amounts to 7823.10 MWh, lower than 8126.47 MWh in method 2 and 8544.77 MWh in method 3, and the prominent loss reduction effect reflects the characteristic of high-efficiency energy use in the regional level EI.

The ASAIs of method 1 and method 2 are greater than that of method 3, mainly because the dual independent bus structure is adopted in region 2, improving the power supply reliability of the entire system. Also, the calculation results of the reliability index in this multi-area case are relatively smaller than those in the single-area case. This is because there is only load, no power sources or energy storage in region 3, so region 1 and region 2 need to supply energy to it through transmission lines, leading to longer power supply distance, higher probability of failure, and larger power interruption range caused by single component failure.

VI. Conclusion

This paper proposes an abstract model of ER and establishes the mapping relationship between network structure and the actual physical layer based on the complex network theory, and finally realizes the design and optimization of power networks of the physical layer of ER. The main conclusions are as follows.

(1) The proposed abstract model of ER has a generic meaning, which can accurately express the functional characteristics of ER and match the actual physical layer design.

(2) The complex network theory can map the power supply and distribution system of ER into complex networks. The improved GN algorithm can reasonably divide nodes into communities and realize the design of IBSs inside ER.

(3) The two cases show that compared with the traditional design scheme, the proposed configuration strategy reduces total cost by 20.68% and 23.39%, and energy loss by 27.98% and 10.54%, respectively, and the designed ER system is more reliable. The proposed method applies to both single-area and multi-area systems.

References

[1] J. Rifkin, The Third Industrial Revolution: How Lateral Power is Transforming Energy, the economy, and the World, New York, NY, USA: Palgrave Macmillan Trade, 2011, pp. 33–72.

[2] S. J. Davis *et al.*, "Net-zero emissions energy systems," *Science*, vol. 360, no. 6369, June 2018.

[3] A. Q. Huang, M. L. Crow, G. T. Heydt, J. P. Zheng, and S. J. Dale, "The Future Renewable Electric Energy Delivery and Management (FREEDM) System: The Energy Internet," *Proc. IEEE*, vol. 99, no. 1, pp. 133-148, Jan. 2011.

[4] H. Zhang, Y. Li, D. W. Gao, and J. Zhou, "Distributed Optimal Energy Management for Energy Internet," *IEEE Trans. Ind. Inform.*, vol.13, no.6, pp.3081-3097, Dec. 2017.

[5] K. L. Zhou, S. L. Yang, and Z. Shao, "Energy Internet: The business perspective", *Appl. Energy*, vol. 178, pp. 212-222, Spet. 2016.

[6] R. P. Kandula, A. Iyer, R. Moghe, J. E. Hernandez, and D. Divan, "Power Router for Meshed Systems Based on a Fractionally Rated Back-to-Back Converter," *IEEE Trans. Power Electron.*, vol. 29, no. 10, pp. 5172-5180, Oct. 2014.

[7] R. Abe, H. Taoka, and D. McQuilkin, "Digital Grid: Communicative Electrical Grids of the Future," *IEEE Trans Smart Grid*, vol. 2, no. 2, pp. 399-410, June 2011.

[8] B. Liu, Y. Peng, J. Xu, C. Mao, D. Wang, and Q. Duan, "Design and Implementation of Multiport Energy Routers Toward Future Energy Inter-net," *IEEE Trans. Ind. Appl.*, vol. 57, no. 3, pp. 1945-1957, May-June 2021.

[9] S. Zhao, Z. Wang, J. Umuhoza, A. Mantooth, Y. Zhao, and C. Farnell, "Distributed power quality enhancement using residential power routers," in *Proc. IEEE Appl. Power Electron. Conf. Expo.* San Antonio, TX, USA, Mar. 2018, pp. 513-520.

[10] L. Yuan, S. Wei, J. Ge, Z. Zhao, and R. Huang, "Design and implementation of AC-DC hybrid multi-port energy router for power distribution networks," in *Proc. 18th Int. Conf. Elect. Mach. Syst.* Pattaya, Thailand, Oct. 2015, pp. 591-596.

[11] P. H. Nguyen, W. L. Kling, and P. F. Ribeiro, "Smart Power Router: A Flexible Agent-Based Converter Interface in Active Distribution Networks," *IEEE Trans. Smart Grid*, vol. 2, no. 3, pp. 487-495, Sept. 2011.

[12] X. She, A. Q. Huang, S. Lukic, and M. E. Baran, "On Integration of Solid-State Transformer With Zonal DC Microgrid," *IEEE Trans. Smart Grid*, vol. 3, no. 2, pp. 975-985, June 2012.

[13] M. R. Sandgani and S. Sirouspour, "Coordinated Optimal Dispatch of Energy Storage in a Network of Grid-Connected Microgrids," *IEEE Trans. Sustain. Energy*, vol. 8, no. 3, pp. 1166-1176, July 2017.

[14] T. Liu, D. Zhang, H. Dai, and T. Wu, "Intelligent Modeling and Optimization for Smart Energy Hub," *IEEE Trans. Ind. Electron.*, vol.66, no.12, pp.9898-9908, Dec. 2019.

[15] N. Zhou *et al.*, "Coordinated planning of multi-area multi-energy systems by a novel routing algorithm based on random scenarios," *Int. J. Elec. Power*, vol. 131, Oct. 2021, Art. no. 107028.

[16] D. Xu, Q. Wu, B. Zhou, C. Li, L. Bai, and S. Huang, "Distributed Multi-Energy Operation of Coupled Electricity, Heating, and Natural Gas Networks," *IEEE Trans. Sustain. Energy*, vol. 11, no. 4, pp. 2457-2469, Oct. 2020.

[17] H. Guo, F. Wang, L. Zhang and J. Luo, "A Hierarchical Optimization Strategy of the Energy Router-Based Energy Internet," *IEEE Trans. Power Syst.*, vol. 34, no. 6, pp. 4177-4185, Nov. 2019.

[18] Y. Chen, P. Wang, Y. Elasser, and M. Chen, "Multicell Reconfigurable Multi-Input Multi-Output Energy Router Architecture," *IEEE Trans. Power Electron.*, vol. 35, no. 12, pp. 13210-13224, Dec. 2020.

[19] P. Li, W. Sheng, Q. Duan, Z. Li, C. Zhu, and X. Zhang, "A Lyapunov Optimization-Based Energy Management Strategy for Energy Hub With Energy Router," *IEEE Trans. Smart Grid*, vol. 11, no. 6, pp. 4860-4870, Nov. 2020.

[20] Y. Liu, X. Chen, Y. Wu, K. Yang, J. Zhu, and B. Li, "Enabling the Smart and Flexible Management of Energy Prosumers via the Energy Router with Parallel Operation Mode," *IEEE Access*, vol. 8, pp. 35038-35047, 2020.

[21] B. Liu *et al.*, "An AC-DC Hybrid Multi-Port Energy Router with Coordinated Control and Energy Management Strategies," *IEEE Access*, vol. 7, pp. 109069-109082, 2019.

[22] S. M. S. Hussain, M. A. Aftab, F. Nadeem, I. Ali and T. S. Ustun, "Optimal Energy Routing in Microgrids With IEC 61850 Based Energy Routers," *IEEE Trans. Indus. Electro.*, vol. 67, no. 6, pp. 5161-5169, June 2020.

[23] E. N. Sosnina, N. V. Shumskii and P. A. Shramko, "Development of a Distributed Energy Router Control System Based on a Neural Network," in *Proc. 2020 Inter. Ural Conf. Elec. Power Eng. (UralCon)*, Chelyabinsk, Russia, Sept. 2020, pp. 313-317.

[24] Y. Xu, J. Zhang, W. Wang, A. Juneja, and S. Bhattacharya, "Energy router: Architectures and functionalities toward Energy Internet," in *Proc. IEEE Int. Conf. Smart Grid Communications*, Brussels, Belgium, Oct. 2011, pp. 31-36.

[25] H. M. Hussain, A. Narayanan, P. H. J. Nardelli, and Y. Yang, "What is Energy Internet? Concepts, Technologies, and Future Directions," *IEEE Access*, vol. 8, pp. 183127-183145, 2020.

[26] S. V. Buldyrev, R. Parshani, G. Paul, H. E. Stanley, and S. Havlin, "Catastrophic cascade of failures in interdependent networks," *Nature*, vol. 464, pp. 1025-1028, Apr. 2010.

[27] J. V. Milanović and W. Zhu, "Modeling of Interconnected Critical Infrastructure Systems Using Complex Network Theory," *IEEE Trans. Smart Grid*, vol. 9, no. 5, pp. 4637-4648, Sept. 2018.

[28] X. Wei, S. Gao, T. Huang, E. Bompard, R. Pi, and T. Wang, "Complex Network-Based Cascading Faults Graph for the Analysis of Transmission Network Vulnerability," *IEEE Trans. Ind. Inform.*, vol. 15, no. 3, pp. 1265-1276, Mar. 2019.

[29] M. Grivan and M. E. J. Newman, "Community structure in social and biological networks," *Proc. Natl. Acad. Sci. U. S. A.*, vol. 99, no. 12, pp. 7821-7826, June 2001.

[30] M. E. J. Newman and M. Girvan, "Finding and evaluating community structure in networks," *Phys. Rev. E*, vol. 69, no. 22, pp. 1-15, Feb. 2004.

[31] B. Stott and O. Alsac, "Fast Decoupled Load Flow," *IEEE Trans. Power App. Syst.*, vol. PAS-93, no. 3, pp. 859-869, May 1974.

[32] A. M. Rei and M. T. Schilling, "Reliability Assessment of the Brazilian Power System Using Enumeration and Monte Carlo," *IEEE Trans. Power Syst.*, vol. 23, no. 3, pp. 1480-1487, Aug. 2008.

[33] D. Krupenev, D. Boyarkin and D. Iakubovskii, "Improvement in the computational efficiency of a technique for assessing the reliability of electric power systems based on the Monte Carlo method," *Reliab. Eng. Syst. Safe.*, vol. 204, 107171, Dec. 2020.

[34] S. Z. Martínez and C. A .C. Coello, "A multi-objective particle swarm optimizer based on decomposition," in *Proc. 13th Annu. Conf. Genetic Evol. Comput. (GECCO)*, July 2011, pp. 69-76.

[35] C. Yue, B. Qu and J. Liang, "A Multiobjective Particle Swarm Optimizer Using Ring Topology for Solving Multimodal Multiobjective Problems," *IEEE Trans. Evol. Comput.*, vol. 22, no. 5, pp. 805-817, Oct. 2018.

[36] F. He, Z. Zhao, and L. Yuan, "Impact of inverter configuration on energy cost of grid-connected photovoltaic systems," *Renew. Energy*, vol. 41, pp. 328-335, May 2012.

[37] T. Wildi, *Electrical Machines, Drives, and Power Systems (6th Edition)*, Pearson Educación, 2006.

[38] B. R. Shrestha, U. Tamrakar, T. M. Hansen, B. P. Bhattarai, S. James, and R. Tonkoski, "Efficiency and Reliability Analyses of AC and 380 V DC Distribution in Data Centers," *IEEE Access*, vol. 6, pp. 63305-63315, 2018.

[39] Y. Lei *et al.*, "A new reliability assessment approach for integrated energy systems: Using hierarchical decoupling optimization framework and impact-increment based state enumeration method," *Appl. Energy*, vol.210, pp.1237-1250, Jan. 2018.

[40] R. Grinberg, G. Riedel, A. Korn, P. Steimer, and E. Bjornstad, "On reliability of medium voltage multilevel converters," in *Proc. IEEE Energy Convers. Congr. Expo. (ECCE)*, Denver, CO, USA, Spet. 2013, pp. 4047-4052.

[41] B. Zhao, H. Qiu, R. Qin, X. Zhang, W. Gu, and C. Wang, "Robust Optimal Dispatch of AC/DC Hybrid Microgrids Considering Generation and Load Uncertainties and Energy Storage Loss," *IEEE Trans. Power Syst.*, vol. 33, no. 6, pp. 5945-5957, Nov. 2018.